catalysts

MDPI

Article

Catalytic Oxidation of Phosphine by Aqueous Copper–Ammonia Complexes

Akbope K. Borangazieva, Yerzhan A. Boleubayev, Zhuldyz U. Ibraimova, Sholpan S. Itkulova * and Gulshara S. Polimbetova

D.V. Sokolsky Institute of Fuel, Catalysis, and Electrochemistry, Almaty 050010, Kazakhstan
* Correspondence: sholpan.itkulova@gmail.com

Abstract: The furnace gas resulting from the electrothermal production of yellow phosphorus contains up to 95% CO, 2% O_2, 2% H_2, and 0.3–4.0% impurities, including phosphine (PH_3), yellow phosphorus (P_4), and hydrogen sulphide (H_2S), which are characterized by flammability, explosion hazardousness, corrosiveness, and high toxicity. The presence of toxic impurities does not allow the use of waste gases from phosphorus production, which are mainly composed of valuable carbon monoxide, as chemical raw materials and/or process fuel. The authors propose a method for the purification of furnace gas from the main toxic component, phosphine, by its oxidisation using aqueous copper–ammonia complexes as a catalyst. This approach allows the cleaning process to be conducted under mild conditions. The degree of purification of the model furnace gas from P components is 90–99%, depending on the process conditions.

Keywords: phosphine; catalytic oxidation; aqueous copper–ammonia complexes; furnace gas of phosphorus production; purification; carbon monoxide; experimental study

Citation: Borangazieva, A.K.; Boleubayev, Y.A.; Ibraimova, Z.U.; Itkulova, S.S.; Polimbetova, G.S. Catalytic Oxidation of Phosphine by Aqueous Copper–Ammonia Complexes. *Catalysts* **2023**, *13*, 271. https://doi.org/10.3390/catal13020271

Academic Editors: Agnieszka Siewniak and Anna Chrobok

Received: 17 November 2022
Revised: 11 January 2023
Accepted: 19 January 2023
Published: 25 January 2023

1. Introduction

The industrial electrothermal production of yellow phosphorus generates large amounts of toxic waste, such as furnace gas, phosphorus sludge, and slag. About 2500–3000 m^3 of tail gases per ton of yellow phosphorus produced are released by electric furnaces. They are the primary sources of air pollution in adjacent cities [1,2]. The furnace gas from phosphorus production contains valuable substances, such as up to 95.0% carbon oxide (CO), hydrogen (H_2), and up to 4% oxygen (O_2);and 0.3–4.0% toxic impurities, such as phosphine (PH_3), yellow phosphorus (P_4), phosphorus oxide (P_2O_5); and acid gases, such as hydrogen sulphide (H_2S) and hydrogen fluoride (HF), that result from side reactions involving water [3,4]. The lack of efficient technologies for removing toxic, flammable, and explosive impurities prevent the use of furnace gas as a process fuel for phosphorus production or as a raw material for conversion into high-value chemical feedstocks, such as synthesis gas (CO + H_2). At present, furnace gas from phosphorus production in Kazakhstan is not recycled and is flared. The processing of large reserves of phosphorus-containing raw materials, the increase in serious air pollution, and more stringent emission standards require the creation of effective methods for removing toxic impurities for further safe utilization of flue gases.

Phosphine is one of the most highly toxic flue gas contaminants. Its high toxicity can cause serious harm to the environment and humans. Various methods can be used to clean flue gases from the electrothermal production of yellow phosphorus from phosphine, including adsorption, oxidation reactions of toxic impurities, catalytic decomposition processes, and electrochemical methods of phosphine removal. Additionally, attempts at bio-treatment to neutralize the tail gas from PH_3 have been made, but their efficiency was not high due to the bio-toxicity of PH_3 [5].

Adsorption methods are used to remove trace amounts of phosphine [6–9]. Among them, materials containing Cu have been widely developed. Thus, zeolites modified

with $CuCl_2$ and $Cu(NO_3)_2$ [7], or $ZnCl_2$ and $CuCl_2$ [8] are reported to be effective. The high sorption capacity for PH_3 of about 130 mg/g for 24 h has been shown by a sorbent composed of coke originating from the Shubarkol deposit (Kazakhstan) modified with additives of CuO (10 wt.%), ZnO (0.1 wt.%), and Cr_2O_3 (1 wt.%) [9].

It should be noted that phosphine is a strong reducing agent, which means that it can be oxidised [10,11]. In fact, breaking the P-H bonds of phosphine requires an electron pair transfer. The two-electron reduction of O_2 to H_2O_2, and the four-electron reduction to H_2O are highly thermodynamically favourable. Despite the high redox potentials of these transitions, the oxidation of PH_3 by oxygen proceeds very slowly under normal conditions since the transfer of an electron pair to an oxygen molecule is impossible due to spin prohibition [11]. However, the oxidation of phosphine may be catalytically accelerated using metal oxides, for example by copper, zinc, chromium, molybdenum oxides, etc. [9,10].

Some new materials for the adsorption and subsequent oxidation of phosphine have been reported. Thus, the walnut-shell-activated carbons demonstrate activity in the oxidation of adsorbed PH_3 to form phosphoric acid (H_3PO_4) and phosphorous oxide (P_2O_5) [12]. The CuO-ZnO-La_2O_3/activated carbon systems with an improved adsorption capacity allow the conversion of adsorbed PH_3 to oxidised forms, such as H_3PO_4 (34.91%) and P_4O_{10} (65.09%) [13]. It has been reported that various metal oxides can be used as adsorbents [14]. Nanocomposites, such as modified CuFe and diatomite (CuFe/MKL), are recognized as the most promising adsorbents for the simultaneous removal of H_2S and PH_3 from gaseous raw acetylene at a low temperature (80 °C) [15]. Tang and colleagues have reported that several metal-containing materials, such as Fe-Ni or Co alloys, are effective for the catalytic decomposition of toxic phosphine to yellow phosphorus and hydrogen [16,17]. A series of oxides of metals, such as Cu, Zn, Mn, and Mo, have been proven to have an excellent PH_3 removal effect [10]. Copper oxides have been reported to be better at removing PH3 and H2S compared to other metal oxides [18]. Copper species can activate oxygen to oxidise reducing gases. Thus, $CuCl_2$ deposited on γ-Al_2O_3 with a large surface area demonstrates a high activity to produce H_3PO_4 and P_2O_5, while the primary γ-Al_2O_3 does not have an adsorption capacity, whereas amorphous $CuCl_2$ shows a high reactivity for the adsorption of PH_3 [19].

In addition to heterogeneous adsorbents and catalysts, absorption and catalysis by homogeneous complex catalysts are of interest due to their high activity, selectivity, and ability to operate under mild conditions. Copper (I, II) complexes are often used in catalysis because they accelerate reactions of completely different natures involving inorganic and organic compounds. While Cu(II) complexes activate addition reactions, Cu(I) complexes accelerate oxidation reactions. Cupric (Cu^{2+}) and cuprous (Cu^{1+}) ions are often used together as a bifunctional catalyst for the activation of various components and stages of the process involving oxygen and oxygen-containing agents [20]. Thus, even though direct oxidation of PH_3 with oxygen is inefficient, catalytic oxidation can occur, for example, in the presence of highly active copper compounds [10,21–24].

We have previously studied complexes of copper with acids (HCl and HBr) in aqueous alcohol solutions. It was shown for the first time that these complexes are promising for use as catalysts for the oxidation of phosphine [21,22]. The acids were later replaced by ammonia to produce a valuable product, such as diammonium phosphate—a mineral fertiliser. Preliminary results were published in [23]. Copper-ammonium complexes were shown to be able to remove phosphine and could be used to purify furnace gas. The present study is aimed at developing this approach and improving the manufacturability of the process. In this regard, the type of reactor was changed from a shaken one to flow one with an overhead stirrer, the volume of the catalytic solution was increased from 10 mL to 100–200 mL, and the effect of conditions was systematically studied. In contrast to the known methods of phosphine removal, the aqueous copper–ammonia complexes were used for the oxidation of PH_3 under mild conditions: low temperatures varied within a range of 30–40 °C and at a pressure level of 1 atm. The reaction products were mono-$NH_4H_2PO_4$) and di-ammonium $(NH_4)_2HPO_4$ phosphates.

2. Results and Discussion

2.1. Testing of Oxidation of Phosphine by Aqueous Copper–Ammonia Complexes

In this study, copper sulphate was used as a source of Cu^{2+} ions. The efficiency of aqueous copper–ammonia complexes for removing phosphine was studied depending on the amounts of copper, ammonia, phosphoric acid, the phosphine concentration, and the process temperature. The phosphine removal efficiency or, in the case of oxidative phosphine conversion, the degree of conversion of X(PH_3), was varied within a range of 80–99%, depending on the reaction conditions. It should be noted that the colour of the solution was varied depending on the copper state and the ratio of copper ions.

Without ammonia, an aqueous solution of copper sulphate with an initial blue colour removed PH_3 from a model PH_3–Ar mixture with a purification degree of no more than 90% (Table 1). This value was maintained for a short period of time (40 min); then, the absorption capacity dropped to 0. The final solution became dark grey. Adding NH_4OH to the solution at 30–50 °C led to intensive absorption of even trace amounts of phosphine. Thus, at t = 50 °C, the addition of 0.65 mol/L of NH_4OH to the catalytic solution containing $CuSO_4$ (C_{CuSO4} = 0.4 mmol/L) increased in the degree of phosphine conversion (X(PH_3), %), which reached 95%. Further increasing the concentration of NH_4OH to 1.3 and 2.6 mol/L reduced the degree of phosphine removal up to 82% and 80%, respectively, while the process duration became longer and reached 1.5 h and 2 h, respectively (Table 1). The initial blue colour of the test solution took on a dark grey hue. These results showed that copper–ammonia complexes were more effective than copper alone.

Table 1. The effect of NH_4OH content on the extent of purification from PH_3 at t = 50 °C, V_{PH3} = 40 mL/min.

Composition of Catalytic Solution, mol/L		Content of PH_3, mg/m^3		Purification, %
$CuSO_4$	NH_4OH	Inlet	Outlet	
0.4	0	18,750	1875.0	90.0
0.4	0.65	18,750	937.5	95.0
0.4	1.3	18,750	3375.0	82.0
0.4	2.6	18,750	3750.0	80.0

An increase in the concentration of copper sulphate, as expected, led to an increase in both the rate of absorption of phosphine and the degree of purification. The degree of purification reached 98–99% when 0.6–0.8 mol/L of $CuSO_4$ was added (Table 2).

Table 2. The effect of $CuSO_4$ content on the extent of purification from PH_3 at t = 50 °C, V_{PH3} = 40 mL/min.

Composition of Catalytic Solution, mol/L		Content of PH_3, mg/m^3		Purification, %
$CuSO_4$	NH_4OH	Inlet	Outlet	
0.2	0.65	18,750	750.0	96.0
0.4	0.65	18,750	937.5	95.0
0.6	0.65	18,750	375.0	98.0
0.8	0.65	18,750	375.0	98.0

A study of the kinetics of the phosphine oxidation reaction was conducted. In these experiments, the flow rate of the PH_3-Ar gas mixture was controlled so that the degree of purification remained at the level of 98–99%. For that, the gas flow rate (V_{PH3}, mL/min) gradually decreased to 0 with the saturation of the catalytic solution by phosphine, which was accompanied by a decrease in the absorption capacity and consequently in the catalytic activity.

In Figure 1 (curves 1–4), the dependence of the reaction rate (W_{PH3}, mmol/L × min) and redox potential (φ, V) on the amount of phosphine absorbed (Q_{PH3}, mmol/L) is presented under the conditions: t = 50 °C, X(PH_3) = 98–99%, C_{PH3}^{in} = 2500, and 10,000 mg/m^3, solution composition (mol/L): NH_4OH—1.3, H_3PO_4—1.9, and varying the amount of

$CuSO_4$ in the range of 0.2–0.6 mol/L. As it is shown, the reaction rate rises with the increasing Cu(II) content (curves 1–4, Figure 1a). The potentiometric curves (1–4) indicating the changes in the ratio of Cu valence state are characterised by plateaus at 0.2~0.25 V (Figure 1b).

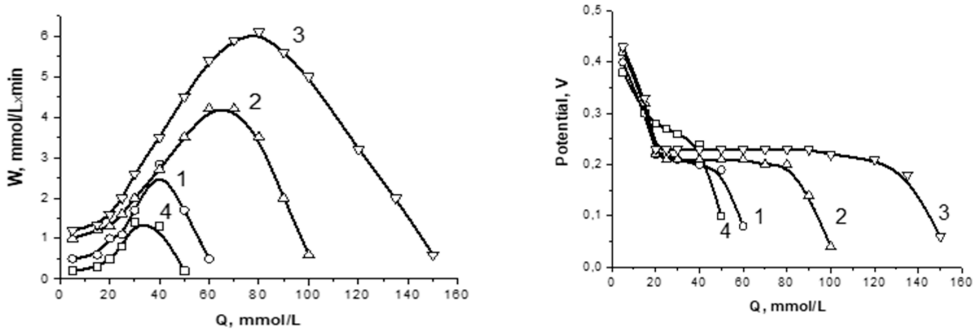

(**a**) (**b**)

Figure 1. Kinetic (**a**) and potentiometric (**b**) curves of PH_3 oxidation by aqueous copper–ammonia complexes at t = 50 °C, X(PH_3) = 98–99%, C_{PH3}^{in} = 10,000 mg/m^3, solution composition, mol/L: NH_4OH—1.3; H_3PO_4—1.9; $CuSO_4$: 0.2 (1), 0.4 (2), 0.6 (3); C_{PH3}^{in} = 2500 mg/m^3, solution composition, mol/L: NH_4OH—1.3; H_3PO_4—1.9; and $CuSO_4$—0.2 (4).

The copper–ammonia catalytic system operated effectively in the low-temperature range of 30–50 °C. Increasing the temperature above 50 °C was accompanied by a decrease in phosphine absorption; hence, PH_3 purification degree from 95–98% to 72%, respectively (Table 3). This may be caused by the destruction of copper–ammonia complexes at rising temperatures.

Table 3. The effect of temperature on the extent of purification from PH_3 at V_{PH3} = 40 mL/min.

Composition of Catalytic Solution, mol/L		t, °C	Content of PH_3, mg/m^3		Purification, %
$CuSO_4$	NH_4OH		Inlet	Outlet	
0.4	0.65	30	18,750	750.0	96.0
0.4	0.65	40	18,750	375.0	98.0
0.4	0.65	50	18,750	937.5	95.0
0.4	0.65	60	18,750	5250.0	72.0

The purification degree depended on the content of phosphine in the gaseous mix. As the concentration of PH_3 in the gas phase increased from 10,000 to 18,750 mg/m^3, the reaction rate increased, and the degree of phosphine removal became higher—96% and 98%, respectively (Table 4).

Table 4. The effect of PH_3 content on the extent of purification from PH_3 at t = 50 °C, V_{PH3} = 40 mL/min.

Composition of Catalytic Solution, mol/L		Content of PH_3, mg/m^3		Purification, %
$CuSO_4$	NH_4OH	Inlet	Outlet	
0.2	0.65	18,750	375.0	98.0
0.2	0.65	10,000	400.0	96.0

Figure 1a demonstrates the dependence of the reaction rate on the content of PH_3 in the gaseous mix. Thus, at a phosphine concentration of 2500 mg/m^3 (curve 4), the rate of reaction is lower than it is at 10,000 mg/m^3 (Figure 1a, curve 1).

It has been observed that the presence of phosphate ions promoted phosphine oxidation (Table 5, Figure 2). Thus, the oxidation degree was increased from 82 to 98% when phosphoric acid was added in an amount of 0.95 mol/L (C_{PH3}^{in} = 18,750 mg/m^3, solution composition, mol/L: NH_4OH—1.3, $CuSO_4$—0.4). The following increase in H_3PO_4 to 1.9 mol/L did not affect the purification degree at various ratios of $CuSO_4/NH_4OH$ (Table 5). A higher purification degree of 99% was achieved in the following conditions: H_3PO_4—1.9 mol/L, C_{PH3}^{in} = 18,750 mg/ m^3, solution composition, mol/L: NH_4OH—1.3, $CuSO_4$—0.6 and NH_4OH—2.6, and $CuSO_4$—0.6.

Table 5. The effect of H_3PO_4 on the PH_3 purification efficiency at t = 50 °C, V_{PH3} = 40 mL/min.

Composition of Catalytic Solution, mol/L			Content of PH_3, mg/m^3		Purification, %
$CuSO_4$	NH_4OH	H_3PO_4	Inlet	Outlet	
0.4	1.3	0	18,750	3375.0	82.0
0.4	1.3	0.95	18,750	375.0	98.0
0.4	1.3	1.9	18,750	375.0	98.0
0.6	1.3	1.9	18,750	187.5	99.0
0.2	2.6	1.9	18,750	187.5	99.0

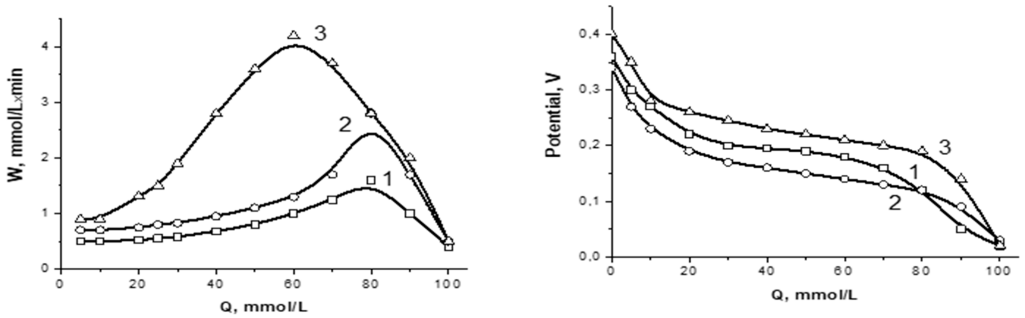

(**a**) (**b**)

Figure 2. Kinetic (**a**) and potentiometric (**b**) curves of PH_3 oxidation by aqueous copper–ammonia complexes at C_{PH3}^{in} = 10,000 mg/ m^3, t = 50 °C, X(PH_3) = 98–99%; solution composition, mol/L: $CuSO_4$—0.4; NH_4OH—1.3; H_3PO_4: 0 (1), 0.95 (2), 1.9 (3).

The significance of phosphoric acid additives is their ability to increase the reaction rate, which is clearly demonstrated in Figure 2a, where the typical kinetic curves of PH_3 absorption are given for copper–ammonia solutions with and without phosphoric acid additives. The rate of phosphine uptake increased by about a factor of two each time H_3PO_4 was added to the catalyst solution (curves 1–3, Figure 2a). As the absorption of PH_3 increased, the reaction rate increased too, reached a maximum, then gradually approached zero (Figure 2a). The potentiometric curves (Figure 2b) indicate the change in the ratio of copper ions—Cu(II)/Cu(I), participating in the reaction. During the reaction, the redox potential of the Cu(II)/Cu(I) pair gradually decreased from 0.4 to 0.1 V, shifted to the cathode side, and reached a relatively steady state which matched the maximum absorption rate of PH_3 on the kinetic curves (Figure 2a), then a sharper drop in potential was observed when the balance between Cu oxidative states disappeared (Figure 2b).

Copper(II) ions form stable complexes with phosphate ions, and the stability constants decrease sharply in the order $PO_4^{3-} \rightarrow HPO_4^{2-} \rightarrow H_2PO_4^{-}$ from $10^7 \rightarrow 10^4 \rightarrow$ and 10^2 [25]. In mixed systems containing ammonia and weak acid anions, acido-amines are formed. Their stability is higher than that of individual acido-complexes and metal amines, and their strength comes close to that of copper(II) complexes with amino acids [26]. In concentrated solutions of ammonia in the absence of phosphate, a low absorption rate of PH_3 was observed (Table 5).

The spent copper–ammonia solution can be regenerated with atmospheric oxygen. After treatment with air (V_{air} = 100 mL/min, t_{amb}), the catalytic solution was quickly regenerated

and restored its initial activity (Table 6, Figure 3). A total of four cycles were conducted; the duration of each cycle was an average of 150 min, and the regeneration time was 50–60 min. After three cycles, the formation of a small amount of white substance was observed. This was monoammonium phosphate, as determined by X-ray diffraction analysis.

Table 6. Stability of catalyst system of $[CuSO_4]$ = 0.4, $[NH_4OH]$ = 0.65, $[H_3PO_4]$ = 0.95 mol/L at t = 30 °C, C_{PH3}^{in} = 2500 mg/m^3.

Number of Cycle	maxW_{ph3}, (mmol/L × min)	Q $_{PH3}$, (mmol/L)	Content of PH_3^{out}, mg/m^3	Purification, %
1	0.5	1.8	50.0	98
2	0.5	1.8	50.0	98
3	0.5	1.7	75.0	97
4	0.5	1.8	100.0	96

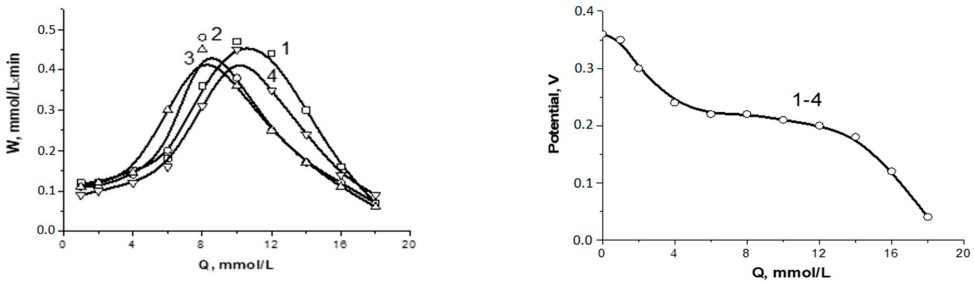

(**a**) (**b**)

Figure 3. Kinetic (**a**) and potentiometric (**b**) curves of PH_3 oxidation by aqueous copper–ammonia complexes at t = 30 °C, C_{PH3}^{in} = 2500 mg/ m^3, X(PH_3) = 98–99%, solution composition, mol/L: NH_4OH—0.65; H_3PO_4—0.95; and $CuSO_4$—0.4; 1–4—cycle number.

After the third cycle, purification degree began to decrease (Table 6). The kinetic curves were close, while the potentiometric curves were completely the same (Figure 3a,b).

2.2. Chemistry of Phosphine Oxidation by Aqueous Copper–Ammonia Complexes

An aqueous solution of $CuSO_4$ consists of hydrated Cu^{2+} ions—$[Cu(H_2O)_6]^{2+}$ that are pale blue in colour. In the interactions of copper(II) ions with ammonia in aqueous medium, aqueous copper–ammonia complexes $[Cu(NH_3)_4(H_2O)_2]^{2+}$ that are ultramarine in colour are formed. The NH_3 ligand forms strong coordination compounds with cupric (2+) or cuprous (1+) ions depending on the anionic ligand [27]. Cuprous ions form stronger complexes with ammonia than cupric ions. Phosphine, such as ammonia, is also prone to complex formation reactions with electron-withdrawing molecules [3,21–23,28–30]. The phosphine ligand-based complexes are widely applied in cross-coupling reactions, asymmetric hydrogenation, hydrocarboxylation, and many other crucially important processes [28].

The catalytic removal of phosphine occurs because of its interaction with the aqueous copper–ammonia complexes accompanied by redox reactions. The resulting chemical reactions of phosphine oxidation with the formation of mono- or diammonium phosphate, depending on the amount of ammonia added, can be generally represented by Equations (1) and (2), respectively:

$$PH_3 + 2O_2 + NH_4OH \rightarrow NH_4H_2PO_4 + H_2O \quad (1)$$

$$PH_3 + 2O_2 + 2NH_4OH \rightarrow (NH_4)_2HPO_4 + 2H_2O \quad (2)$$

The formation of monoammonium phosphate (Equation (1)) is confirmed by an XRD analysis of a white powder collected at the end of the process. The observed reflections of

5.33, 3.76, 3.08, 2.65, 2.38, 2.01, 1.77, 1.68, 1.60, 1.47, 1.37, 1.32, 1.25, 1.21, and 1.18 correspond to monoammonium phosphate—$NH_4H_2PO_4$ (ASTM 1-817) (Figure 4).

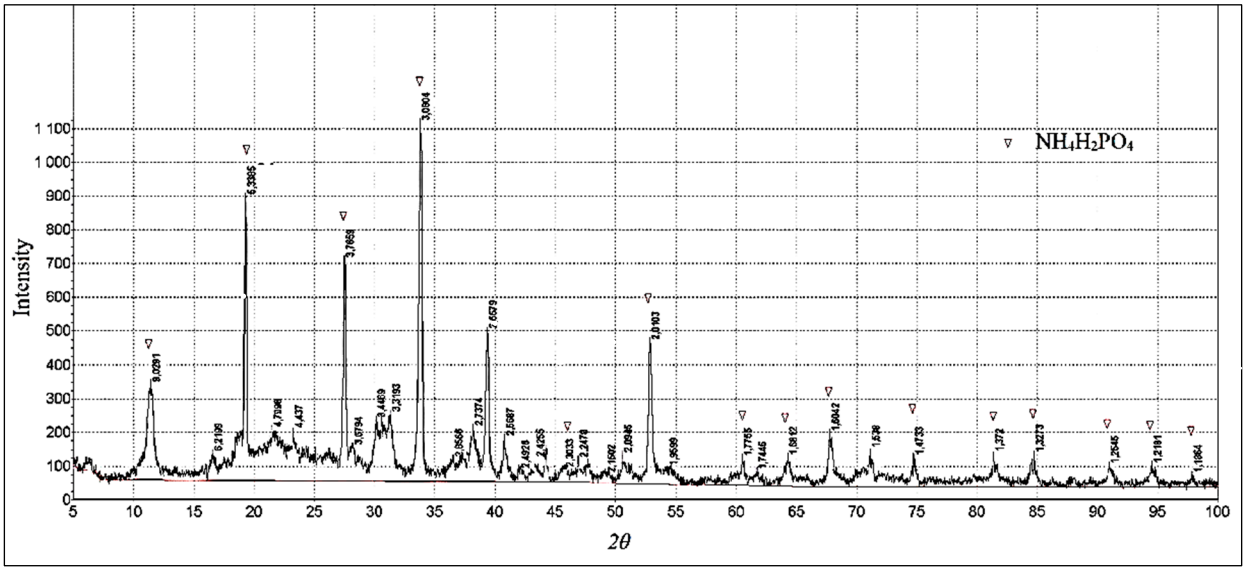

Figure 4. XRD pattern of the product of PH_3 oxidation by aqueous copper–ammonia complexes; labels refer to reflections attributed to monoammonium phosphate—$NH_4H_2PO_4$ (ASTM 1-817).

The copper complexes act as a catalyst can be described by the following consecutive redox reactions: phosphine oxidation, $P^{3-} \rightarrow P^{5+}$, and copper reduction, $Cu^{2+} \rightarrow Cu^0$, (Equation (3)); the formation of copper(I) (Equation (4)); and oxidation of copper(I) by oxygen and return to an initial Cu(II) state (Equation (5)).

$$PH_3 + 4Cu^{2+}X + 9NH_4OH \rightarrow NH_4H_2PO_4 + 4Cu^0 + 4(NH_4)_2X + 5H_2O \quad (3)$$

$$Cu^0 + Cu^{2+}X \leftrightarrow (Cu^{1+})_2X \quad (4)$$

$$(Cu^{1+})_2X + 1/2O_2 + (NH_4)_2X + H_2O \rightarrow 2Cu^{2+}X + 2NH_4OH \quad (5)$$

where $X = SO_4^{2-}$. In contrast to Cu(II) ions, the catalytic effect of Cu(I) ions is the tendency to form complexes with phosphine [11,21,22]. Without copper(I) ions, the copper(II) ions do not react with PH_3, and phosphine does not reduce the Cu(II) ions. The process is started with the stage of formation of Cu(I) phosphide complexes. Then, the Cu(II) phosphide undergoes redox decomposition with the release of phosphine oxide and Cu(0). The accumulation of metallic copper is accompanied by a lack of Cu(II), and a decrease in the absorption of phosphine. With an excess of Cu(II), the equilibrium (Equation (6)) is shifted to the right [25,26]. The same approach with Cu ions playing a leading role in removing H_2S and PH_3 is postulated by the authors of [3].

$$Cu^{2+}(NH_3)_2(HPO_4) + Cu^0 + H_3PO_4 + 2NH_4OH \leftrightarrow 2Cu^{1+}(NH_3)_2(H_2PO_4) + 2H_2O \quad (6)$$

X-ray analysis proves that the formation of Cu^0 appeared as a black powder on the inner wall of the reactor. The reflections at 2.09, 1.81, and 1.28, respectively, are attributed to Cu^0 (ASTM 4-0836) (Figure 5). The SEM pattern of the black precipitation corresponding to Cu^0 is presented in Figure 6.

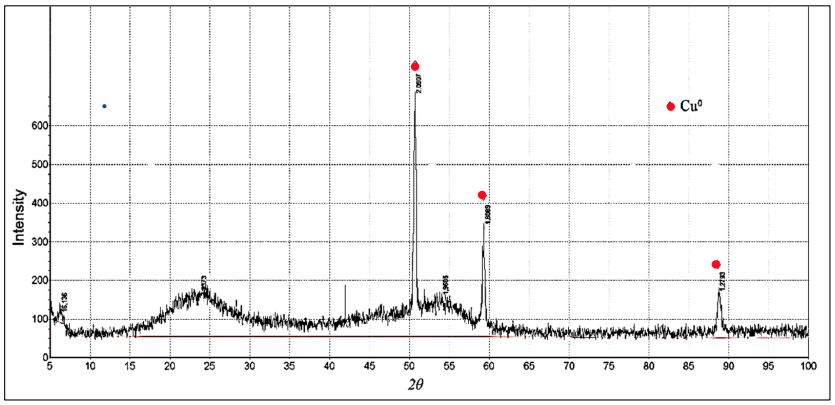

Figure 5. XRD pattern of the precipitation formed during phosphine oxidation by aqueous copper–ammonia complexes; labelled peaks at 2.09, 1.81, and 1.28 attributed to Cu^0 (ASTM 4-0836).

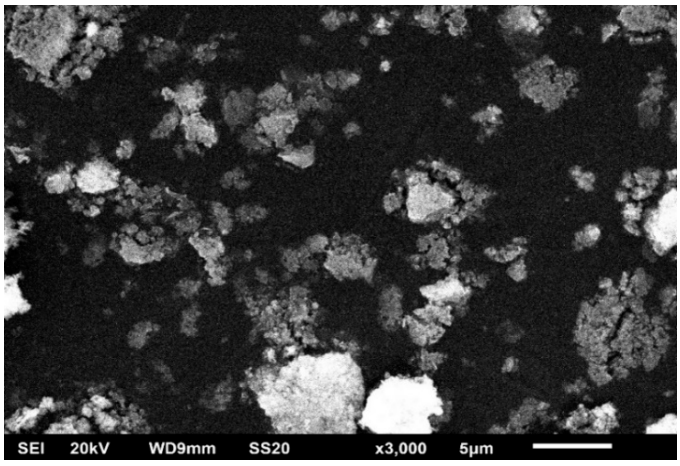

Figure 6. SEM pattern of Cu^0-containing precipitation.

Copper ions do not react with mono/diammonium phosphate; as a result of the reaction, mono/diammonium phosphate (ammophos) suitable for use as a complex mineral fertilizer is formed. The main elements included in ammonium phosphates and Cu^0, such as N, O, P, and Cu, with an average content of 15.25, 51.55, 25.7, and 6.69 wt.%, respectively, were detected using the EDX-SEM analysis of residues collected after five cycles of the process of phosphine oxidation and drying at ambient temperature (Figure 7).

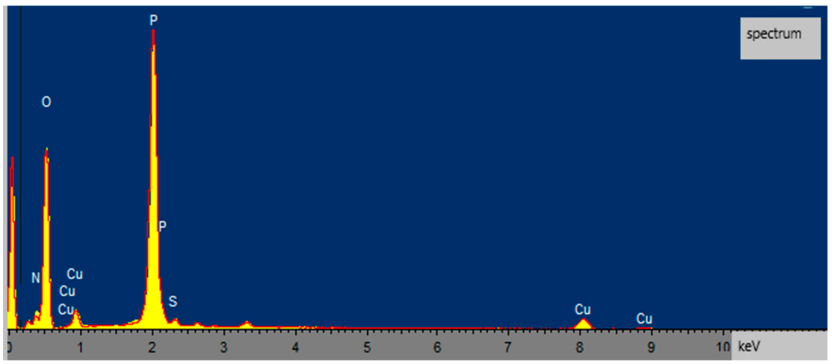

Figure 7. SEM-EDX analysis of residues collected after five cycles of phosphine oxidation.

Since the oxidation of phosphine by aqueous copper–ammonia complexes were accompanied by a change in the oxidation states of copper (Equations (3)–(5)), measurements

of the redox potential were conducted. Figure 8 illustrates the dependence of the phosphine conversion (X_{PH3}, %) and redox potential (φ, V) on time.

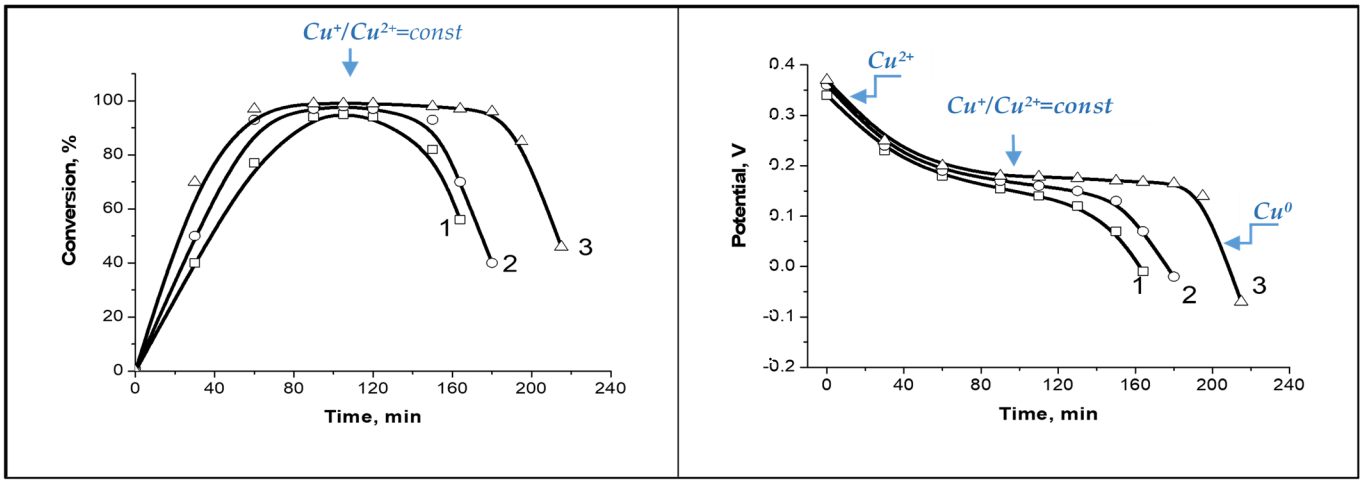

(**a**) (**b**)

Figure 8. Conversion (**a**) and potentiometric (**b**) curves of PH_3 absorption at 40 °C, V_{PH3} = 40 mL/min, PH_3—493 mg/m^3, composition, mol/L: NH_4OH—0.65, $CuSO_4$—0.02 (curve 1), 0.04 (curve 2), and 0.06 (curve 3).

The potentiometric curves (1–3) (Figure 8b) are characterised by a decrease in the value of redox potential at the beginning of the reaction, with plateaus arising at φ ~ 0.2 V, and a new sharp drop in redox potential at the end of the reaction. A drop in the redox potential corresponds to a change in oxidative states of Cu while the plateau indicates the establishment of equilibrium Cu(I)/Cu(II). The first drop corresponds to a transition of Cu(II) to the Cu(I) state, while the second one indicates the further reduction of Cu and the formation and accumulation of Cu(0), which is not active for phosphine oxidation and should be oxidised to return to an initial Cu^{2+} state. The plateau corresponds to Cu(I)/Cu(II) equilibrium.

Along the conversion curves, the plateau arises at the same time as the potentiometric curves, when the Cu(I)/Cu(II) equilibrium is established (Figure 8a). The longer the plateau, the higher the amount of absorbed phosphine, and the longer the duration of the process. The falling redox potential is accompanied by a decrease in the reaction rate up to 0 due to an increase in the Cu(0) amount, and its visible accumulation since the solution's colour changes, and a black precipitate form. Thus, the redox potential is useful to monitor the changes in the catalytic system. The presence of plateaus on potentiometric curves is evidence of the stable work of the catalytic system possessing a higher absorption capacity and depth of oxidation.

Thus, summarizing the results obtained, we propose that the oxidation of PH_3 by an aqueous copper–ammonia solution consists of three key steps: (1) reduction of copper(II) to metallic copper (Cu(0)) by phosphine—as a result of the redox process, mono- or diammonium phosphates are formed (Equation (3)); (2) oxidation of Cu(0) by Cu(II) to Cu(I) (Equation (4)); and (3) oxidation of Cu(I) by oxygen and the regeneration of the initial copper state (Cu(II)). The first stage is accelerated by copper(I), while the last stage is accelerated by copper(II).

The resulting Cu(0) is oxidised by O_2 to the ammoniates Cu(I) and Cu(II) Equation (7)). Under the action of oxygen, copper(I) is reoxidised to copper(II) and returned to the catalytic cycle (Equation (8)).

$$2Cu + 2(NH_4)_2HPO_4 + O_2 \rightarrow 2Cu(NH_3)_2(H_2PO_4) + 2H_2O \quad (7)$$

$$4Cu(NH_3)_2(H_2PO_4) + O_2 \rightarrow 4Cu(NH_3)_2(HPO_4) + 2H_2O \quad (8)$$

3. Materials and Methods

3.1. Materials

Gas (Ar) of 99.99% purity was supplied from a gas cylinder. Phosphine was obtained by the decomposition of zinc phosphide (Equation (9)).

$$Zn_3P_2 + 3H_2SO_4 \rightarrow 2PH_3 + 3ZnSO_4 \quad (9)$$

All reagents used met the established standards (Kazakhstan) and had a purity of at least 99%.

The phosphoric acid (H_3PO_4) concentration was 85%, GOST 6552-80, JSC "Reaktiv", Novosibirsk, Russia.

The aqueous ammonia (NH_4OH) concentration was 25%, GOST 3760-79, LLP "LabChemProm", Russia.

The zinc phosphide (Zn_3P_2) contained 19% phosphorus, Sigma-Aldrich GmbH, Germany.

The copper sulphate pentahydrate ($CuSO_4$*$5H_2O$, 99.5%), GOST 4165-78, "JSC REAHIM" Russia.

3.2. Preparation of Phosphine

Phosphine was obtained by acid decomposition of Zn_3P_2 according to Equation (9).

The produced PH_3 was carried by an argon stream into graduated bottles (gasometer) filled with saturated NaCl solution. Then, phosphine was diluted with argon to obtain a certain content of phosphine that varied within 0.2–1.6 vol.%, corresponding to 2500–18,750 mg/m^3.

3.3. Preparation of Aqueous Copper–Ammonia Solution

A solution of $CuSO_4$ with a concentration varied within 0.2–0.6 mol/L was prepared by dissolving the salt in distilled water. The final solution consisting of $[Cu(H_2O)_6]^{2+}$ ions was blue in colour. Then, 0.65–2.6 mol/L of NH_4OH was added to the solution. The initial blue colour of the solution changed to blue-violet. This indicates the formation of copper–ammonia complexes $[Cu(NH_3)_4(H_2O)_2]^{2+}$ ions, usually written as $[Cu(NH_3)_4]^{2+}$ ion. Ammonia is a stronger base than H_2O, and therefore displaces the water molecules from the hydrated Cu^{2+} ion [31]. Finally, phosphoric acid is added to the catalytic solution in the amount of 0.95–1.9 mol/L, and the colour of the solution became ultramarine. The catalytic solution was purged with Ar and the redox potential and pH were measured. The optimal values of the pH and redox potential are 6.5–7 and 65–70 mV, respectively.

3.4. Testing

The processes of absorption and oxidation of PH_3 by a catalytic solution were conducted in a flow thermostatic unit with inputs and outputs comprising gaseous, solid, and liquid reagents, and equipped with a device for measuring redox potential and pH values (ionometer—I-160 MI, 2021, Russia, consisting of a redox measuring electrode and a silver chloride reference electrode), an overhead stirrer, and combined lines of the Ar-PH_3 gas mixture and Ar-O_2 supplied from gasometers, which were passed with a certain rate regulated by rotameters/gas flow meters.

The solvent and solid or dissolved catalytic system components with a total volume of 100 mL were placed in a glass reactor (1), which was purged with argon before supplying the model gas mixture; the catalytic solution was stirred using an overhead stirrer (2, 4) with a rotation frequency of 800 rpm and heated to the test temperature using a thermostat (3); the redox potential was measured, and the gas mixture was passed with a certain flow rate that varied within a range of 30–100 mL/min (Figure 9).

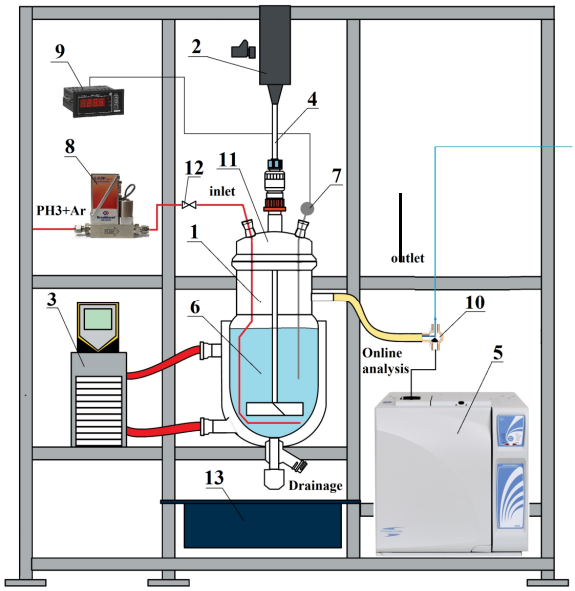

Figure 9. Scheme of a unit for oxidation of phosphine by aqueous copper–ammonia complexes. 1 —glass reactor, V = 0.2 L; 2—overhead drive motor; 3—thermostat; 4—stirrer; 5—gas chromatograph; 6—catalyst solution; 7—electrode; 8—gas flow meter; 9—ion meter and pH-meter; 10—three-way valve; 11—reactor cover; 12—faucet with sampler; and 13—pallet.

At a constant-velocity phosphine feed (V_{PH3}), eventually, the catalytic solution was saturated with phosphine, leading to a decrease in the absorption rate and the degree of purification. To conduct kinetic measurements, the phosphine feed velocity was adjusted in such a way as to keep the degree of purification constant (98–99%); for this purpose, the velocity of phosphine was gradually reduced up to 0, i.e., until the processes of absorption and oxidation in phosphine had completely stopped.

During the experiment, the redox potential (V), absorption rate of PH_3 (W, mol/L min), and amount of absorbed PH_3 (Q, mol/L) at a given time were measured online. The concentration of phosphine before and after absorption was determined online by GC. The experiments were conducted until the absorption of PH_3 had almost stopped.

Regeneration of the spent experimental solution was conducted in the same reactor and pre-blown with argon, then with air at a rate of 20–30 mL/min for 30–60 min. Air was generated by an air compressor, "GChV–1.2-3.5", 2017, Russia.

3.5. Analysis of Products and Calculation Methods

The concentrations of PH_3 in the initial gas feed (before reactor), and outgoing gases (after reactor) were analysed using the online gas chromatograph "Chromatec–Crystal 5000" with a DTP detector with the software "Chromatec Analytic", made in Russia, 2020; packed column: NaX 80/100 mesh; capillary column: PoraPLOT Q. Carrier gases with a purity of 99.9%–argon for the packed column and helium for the capillary column were supplied from cylinders. Sampling was performed with a 6-port tap (automatic, thermostatically controlled) with a 0.5 mL and 1.0 mL dosage.

The solid product composition was analysed by means of X-ray diffraction (XRD) using a "Dron-4" powder diffractometer (USSR, 1990) with the CuK_α or CoK_α radiation upgraded and equipped with software processing. The phase identification was performed with the help of the ASTM (American Society for Testing and Materials).

Scanning electron microscopy (SEM) images were taken using JSM 6610 LV JOEL equipment using a secondary electron detector operating under high and low vacuum conditions (Japan, 2013).

The removal efficiency or degree of purification from phosphine (X_{PH3}) was calculated according to Formula (10):

$$X_{PH3} = ((C_{PH3}{}^{in} - C_{PH3}{}^{out})/C_{PH3}{}^{in}) \times 100\% \quad (10)$$

where $C_{PH3}{}^{in}$ is the concentration of phosphine in the feed mixture, and $C_{PH3}{}^{out}$ is the concentration of phosphine in the outlet mixture.

Parameters, such as the duration (τ, min), redox potential (φ, V), rate of absorption of PH_3 (W, mmol/L×min), and amount of absorbed PH_3 (Q, mmol/L), were measured. The composition of the gas phase was analysed online. The kinetic test was conducted until PH_3 did not stop being absorbed by the catalytic solution. The process rate was assessed by the consumption of PH_3 and the accumulation of the product.

The rate of phosphine absorption—W_{PH3}, mol/(L×min) and quantity of absorbed phosphine—Q, mol/L have been calculated according to Formulas (11) and (12), respectively:

$$W_{PH3} = V_{PH3} \times (C_{PH3}{}^{in} - C_{PH3}{}^{out})/(V_l \times M_{PH3}) \quad (11)$$

$$Q_{PH3} = V_{PH3} \times (q_{PH3}{}^{in} - q_{PH3}{}^{out})/(V_l \times M_{PH3}) \quad (12)$$

where V_{PH3} is the volume of gas passed through the catalytic solution; L/min, $C_{PH3}{}^{in}$, and $C_{PH3}{}^{out}$ are concentrations of phosphine in the inlet and outlet gas flows, g/L; V_l is the volume of the liquid catalytic solution, L; q is the quantity of absorbed phosphine, L/mol; and M_{PH3} is the molecular mass of phosphine, g/mol. On the basis of data on W_{PH3}, Q_{PH3}, and potentials, the conversion and potentiometric curves were plotted.

For the usual flow regime, the process was conducted at a certain velocity of gases PH_3 and O_2 (V_g, L/min), which were controlled by mass flowmeters, 2019, Bronkhorst, the Netherlands.

4. Conclusions

The catalytic oxidation of PH_3 by aqueous copper–ammonia complexes under mild conditions has been studied. The process was conducted under atmospheric pressure and low temperatures in the range of 30–50 °C. Such mild conditions avoid parallel chemical transformations of the main component of furnace gas—carbon monoxide.

The studied aqueous copper–ammonia complexes are effective for purification from phosphine; the degree of purification is varied within 90–99% depending on the amount of copper, ammonia, phosphoric acid, and the phosphine concentration in the gas mixture and the temperature.

The main products of a phosphine oxidation reaction are mono- or diammonium phosphate depending on the amount of ammonia added. Both products are valuable fertilizers.

The chemistry of the process is proposed and described. The possible reactions include the reduction of Cu^{2+} to Cu^0, formation of Cu^+ ions, and the regeneration of an initial Cu(II) state.

The developed catalytic system is inexpensive and effective for combating air pollution and utilizing hazardous waste, such as PH_3.

Further studies will be conducted using real furnace gas consisting of carbon monoxide, and a number of impurities in order to find out their effect on the catalytic oxidation of PH_3, and to scale up the process. Additionally, the mechanism of the process will be considered based on additional results.

Author Contributions: Conceptualization, G.S.P.; methodology, A.K.B. and Y.A.B.; software and visualization. Y.A.B.; formal analysis and validation, A.K.B., Z.U.I., S.S.I. and Y.A.B.; investigation and data curation, A.K.B., Y.A.B. and Z.U.I.; resources, Y.A.B. and S.S.I.; writing—original draft preparation, Z.U.I., A.K.B. and Y.A.B.; writing—review and editing, S.S.I. and G.S.P.; supervision, project administration, and funding acquisition, G.S.P. and S.S.I. All authors have read and agreed to the published version of the manuscript.

Funding: This research was funded by the Science Committee of the Ministry of Education and Science of the Republic of Kazakhstan, grant number AP08855848.

Data Availability Statement: Not applicable.

Acknowledgments: The authors wish to thank the Physico-Chemical Methods of the Catalyst Analysis of IFCE for providing the X-ray and SEM analysis of the obtained product.

Conflicts of Interest: The authors declare no conflict of interest. The funders had no role in the design of the study; in the collection, analyses, or interpretation of data; in the writing of the manuscript; or in the decision to publish the results.

References

1. Zhou, Z.; Gao, H. Experimental Study on Combustion Characteristic of Yellow Phosphorus Tail Gas. *Energy Procedia* **2012**, *16*, 763–768. [CrossRef]
2. Ma, J.; Chen, W.; Niu, X.; Fan, Y. The relationship between phosphine, methane, and ozone over paddy field in Guangzhou, China. *Glob. Ecol. Conserv.* **2019**, *17*, e00581. [CrossRef]
3. Bao, J.; Wang, X.; Li, K.; Wang, F.; Wang, C.; Song, X.; Sun, X.; Ning, P. Reaction Mechanism of Simultaneous Removal of H_2S and PH_3 Using Modified Manganese Slag Slurry. *Catalysts* **2020**, *10*, 1384. [CrossRef]
4. Xueqian, W.; Ping, N.; Wei, C. Studies on purification of yellow phosphorus off-gas by combined washing, catalytic oxidation, and desulphurization at a pilot scale. *Sep. Purif. Technol.* **2011**, *80*, 519–525. [CrossRef]
5. Ting, L.; Shugen, L.; Xiaofei, Y. Addition of reactive oxygen scavenger to enhance PH_3 biopurification: Process and mechanism. *Process Saf. Environ. Prot.* **2020**, *142*, 118–125. [CrossRef]
6. Habibi-Yangjeh, A.; Basharnavaz, H.; Kamali, S.H.; Nematollahzadeh, A. A first-principles investigation of PH_3 gas adsorption on the graphitic carbon nitride sheets modified with V/P, Nb/P, and Ta/P elements. *Mater. Chem. Phys.* **2021**, *269*, 124–282. [CrossRef]
7. Xu, X.; Huang, G.; Qi, S. Properties of AC and 13X zeolite modified with $CuCl_2$ and $Cu(NO_3)_2$ in phosphine removal and the adsorptive mechanisms. *J. Chem. Eng.* **2017**, *316*, 563–572. [CrossRef]
8. Xu, X.; Huang, G. Effect of 13X Zeolite Modified with $CuCl_2$ and $ZnCl_2$ for Removing Phosphine from Circular Hydrogen of a Polysilicon Chemical Vapor Deposition Stove. *Ind. Eng. Chem. Res.* **2016**, *55*, 1380–1386. [CrossRef]
9. Gosteva, A.N.; Efremov, S.A.; Nikolaev, V.G. Catalytic Carbon-Containing Composition for Phosphine Oxidation. *Mater. Sci. Eng.* **2021**, *1079*, 062014. [CrossRef]
10. Feng, J.; Wang, F.; Wang, C.; Li, K.; Sun, X.; Ning, P. Cu/HZSM-5 Sorbent Treated by NH3 Plasma for Low-Temperature Simultaneous Adsorption−Oxidation of H_2S and PH_3. *ACS Appl. Mater. Interfaces* **2021**, *13*, 24670−24681. [CrossRef] [PubMed]
11. Dorfman, Y.A. *Liquid Phase Catalysis*; Science of KazSSR: Almaty, Kazakhstan, 1981; p. 364. (In Russian)
12. Yu, Q.; Li, M.; Ning, P.; Yi, H.; Tang, X. Characterization of Metal Oxide-modified Walnut-shell Activated Carbon and Its Application for Phosphine Adsorption: Equilibrium, Regeneration, and Mechanism Studies. *J. Wuhan Univ. Technol. Mater.* **2019**, *34*, 487–495. [CrossRef]
13. Yi, H.; Yu, Q.; Tang, X.; Ning, P.; Yang, L.; Ye, Z.; Song, J. Phosphine Adsorption Removal from Yellow Phosphorus Tail Gas over CuO−ZnO−La_2O_3/Activated Carbon. *Ind. Eng. Chem. Res.* **2011**, *50*, 3960–3965. [CrossRef]
14. Ma, L.; Ning, P.; Zhang, Y.; Wang, X.Q. Experimental and modelling of fixed-bed reactor for yellow phosphorous tail gas purification over impregnated activated carbon. *J. Chem. Eng.* **2016**, *137*, 471–479. [CrossRef]
15. Li, S.; Hao, J.; Ning, P.; Wang, C.; Li, K.; Tang, L.; Sun, X.; Zhang, D.; Mei, Y.; Wang, Y. Preparation of Cu-Fe nanocomposites loaded diatomite and their excellent performance in simultaneous adsorption/oxidation of hydrogen sulfide and phosphine at low temperature. *Sep. Purif. Technol.* **2017**, *180*, 23–35. [CrossRef]
16. Tang, X.; Xue, J.; Xing, C. Catalytic decomposition of toxic phosphine gas on the developed nickel ferrite nanocrystals supported by Halloysite nanotubes. *Appl. Surf. Sci.* **2020**, *530*, 147–264. [CrossRef]
17. Tang, X.J.; Xiu, Z.; Han, C.; Zhang, B. Toxic PH_3 Catalytic Decomposition and High Purity Phosphorus Production by Amorphous Co-Based Alloy Nanomaterials. *ACS Symp. Ser.* **2013**, *11*, 181–199. [CrossRef]
18. Wang, Y.; Lin, Q.; Ning, P.; Wang, C.; Sun, X.; Li, K. Preparation of Ce0.6. Cu60/Al40-[O] Catalyst and Role of CeO_2/CuO in Simultaneous Removal of H_2S and PH_3. *J. Taiwan Inst. Chem. Eng.* **2018**, *87*, 44–53. [CrossRef]
19. Zhou, Y.; He, T.; Liu, S.; Huang, G. Adsorption of Trace Phosphine in Circular Hydrogen of a Polysilicon Chemical Vapor Deposition Stove by Cu/γ-Al_2O_3. *Ind. Eng. Chem. Res.* **2018**, *57*, 15122–15131. [CrossRef]
20. Temkin, O.N. *Homogeneous Metal Complex Catalysis. Kinetic Aspects*; ICC "Akademkniga": Moscow, Russia, 2008; p. 918. (In Russian) [CrossRef]
21. Polimbetova, G.S.; Borangazieva, A.K.; Ibraimova, Z.U.; Bugubaeva, G.O.; Keyinbai, S. Oxidative alkoxylation of phosphine in alcohol solutions of copper halides. *Russ. J. Phys. Chem. A* **2016**, *90*, 1539–1544. [CrossRef]
22. Polimbetova, G.S.; Borangazieva, A.K.; Ibraimova, Z.U.; Ergozhin, E.E.; Mukhitdinova, B.A. Oxidative hydroxylation of phosphine in aqueous alcohol solutions of *p*-benzoquinone. *Russ. J. Phys. Chem. A* **2014**, *88*, 764–767. [CrossRef]
23. Ibraimova, Z.U.; Polimbetova, G.S.; Borangazieva, A.K.; Itkulova, S.S.; Boleubaev, E.A. Catalytic purification and ways for utilization of furnace gas of phosphorus production. *Rep. NAS RK* **2021**, *5*, 136–143. [CrossRef]
24. Ren, Z.; Quan, S.; Zhu, Y.; Chen, L.; Deng, W.; Zhang, B. Purification of Yellow Phosphorus Tail Gas for the Removal of PH_3 on the Spot with Flower-Shaped CuO/AC. *RSC Adv.* **2015**, *5*, 29734–29740. [CrossRef]

25. Kravtsov, V.I. *Equilibrium and kinetics of electrode reactions of metal complexes*; Chemistry Publ., USSR: Moscow, Russia, 1985; p. 208. (In Russian)
26. Hartley, F.; Berges, K.; Alcock, R. *Equilibrium in Solution*; Mir: Moscow, Russia, 1983; p. 345. (In Russian)
27. Velásquez-Yévenes, L.; Ram, R. The aqueous chemistry of the copper-ammonia system and its implications for the sustainable recovery of copper. *Clean. Eng. Technol.* **2022**, *9*, 100515. [CrossRef]
28. Demchuk, O.M.; Jasinski, R.; Strzelecka, D.; Dziuba, K.; Kula, K.; Chrzanowski, J.; Krasowska, D. A clean and simple method for deprotection of phosphines from borane complexes. *Pure Appl. Chem.* **2018**, *90*, 49–62. [CrossRef]
29. Gusarova, N.K.; Verkhoturova, S.L.; Kazantseva, T.L.; Mikhailenko, V.L.; Arbuzova, S.N.; Trofimov, B.A. Free-radical addition of phosphine to vinyl ethers: Atom-economic synthesis of tris(2-organyloxyethyl) phosphines and their derivatives. *Mendeleev Commun.* **2011**, *21*, 17–18. [CrossRef]
30. Librando, I.L.; Mahmoud, A.G.; Carabineiro, S.A.C.; Guedes da Silva, M.F.C.; Geraldes, C.F.G.C.; Pombeiro, A.J.L. The Catalytic Activity of Carbon-Supported Cu(I)-Phosphine Complexes for the Microwave-Assisted Synthesis of 1,2,3-Triazoles. *Catalysts* **2021**, *11*, 185. [CrossRef]
31. Averill, B.A.; Eldredge, P. *General Chemistry: Principles, Patterns, and Applications*; Saylor Academy: Washington, DC, USA, 2012; Volume 14.